Vibrational Analysis of Glutathione

WEILI QIAN and SAMUEL KRIMM

Biophysics Research Division and Department of Physics, University of Michigan, Ann Arbor, Michigan 48109

SYNOPSIS

Infrared and Raman spectra have been obtained of crystalline glutathione and its deuterated derivative and interpreted by normal mode analysis. The force field consisted of our empirical force fields for the peptide group and NH_3^+ and CO_2^- end groups, plus our ab initio force fields for the CH_2SH and CH_2COOH moieties. Observed bands are reproduced with an average error of 5 cm^{-1}, demonstrating that the vibrational spectrum of such a complex molecule can be understood in great depth. © 1994 John Wiley & Sons, Inc.

INTRODUCTION

Glutathione, γ-glutamyl-cysteinyl-glycine, γ-glu-cys-gly (GSH), is an important constituent of living cells.[1] Its major function is to be involved enzymatically in the reduction of hydrogen peroxide and other peroxides, and in general to protect cell components against oxidation.[1,2]

GSH has therefore been the subject of much structural and spectroscopic studies. The crystal structure was first reported by Wright[3] and subsequently redetermined to higher accuracy by Görbitz.[4] Infrared and Raman spectra have been recorded,[5] but no detailed assignments have been made. Conformational and dynamic properties have been studied by nmr,[6] and quantum mechanical calculations of conformation have been attempted.[7]

Our aim was to provide a detailed analysis and assignment of the vibrational spectrum of the crystalline form of GSH. This can enable a deeper understanding of spectra–structure correlations for other structural states of GSH. We have performed normal mode calculations on GSH and its N, S, and O deuterated derivative, GSD, and compared these results with ir and Raman spectra of these compounds. The force field was based on our empirical force fields for the peptide chain[8] and NH_3^+ and CO_2^- end groups,[9-11] and on ab initio force fields for the Cys CH_2SH[12] and Gly CH_2COOH[13] parts of the molecule. The good agreement obtained between observed and calculated frequencies not only validates the empirical peptide force field,[8] as did previous calculations on peptides,[9-11] but it demonstrates that the vibrational spectrum of a molecule as complex as GSH can be understood in great depth.

EXPERIMENTAL PROCEDURES

GSH was obtained from Sigma Chemical Co. We assume that this polycrystalline material has the same structure as the only reported crystal structure of GSH.[3,4] The deuterated derivative was prepared by dissolving GSH in D_2O, evaporating the solution in vacuo for 24 h and repeating the procedure until the NH and SH stretch bands disappeared in the Raman spectrum.

Infrared spectra, at 2 cm^{-1} resolution, were obtained on KBr pellets, using a Bomem DA-3 FTIR spectrometer, and are shown in Figure 1. Raman spectra, at 2 cm^{-1} resolution, were obtained on the powder, using a Spex 1403 spectrometer and Ar^+ laser 514.5 nm excitation, and are shown in Figure 2.

NORMAL MODE CALCULATIONS

Structure

The unit cell of GSH is orthorhombic, with a = 5.622 Å, b = 8.781, Å, and c = 28.023 Å, the space group is $P2_12_12_1$, and Z = 4.[4] The molecular packing is shown in Figure 3. The molecules have fractional

Biopolymers, Vol. 34, 1377–1394 (1994)

CCC 0006-3525/94/101377-18

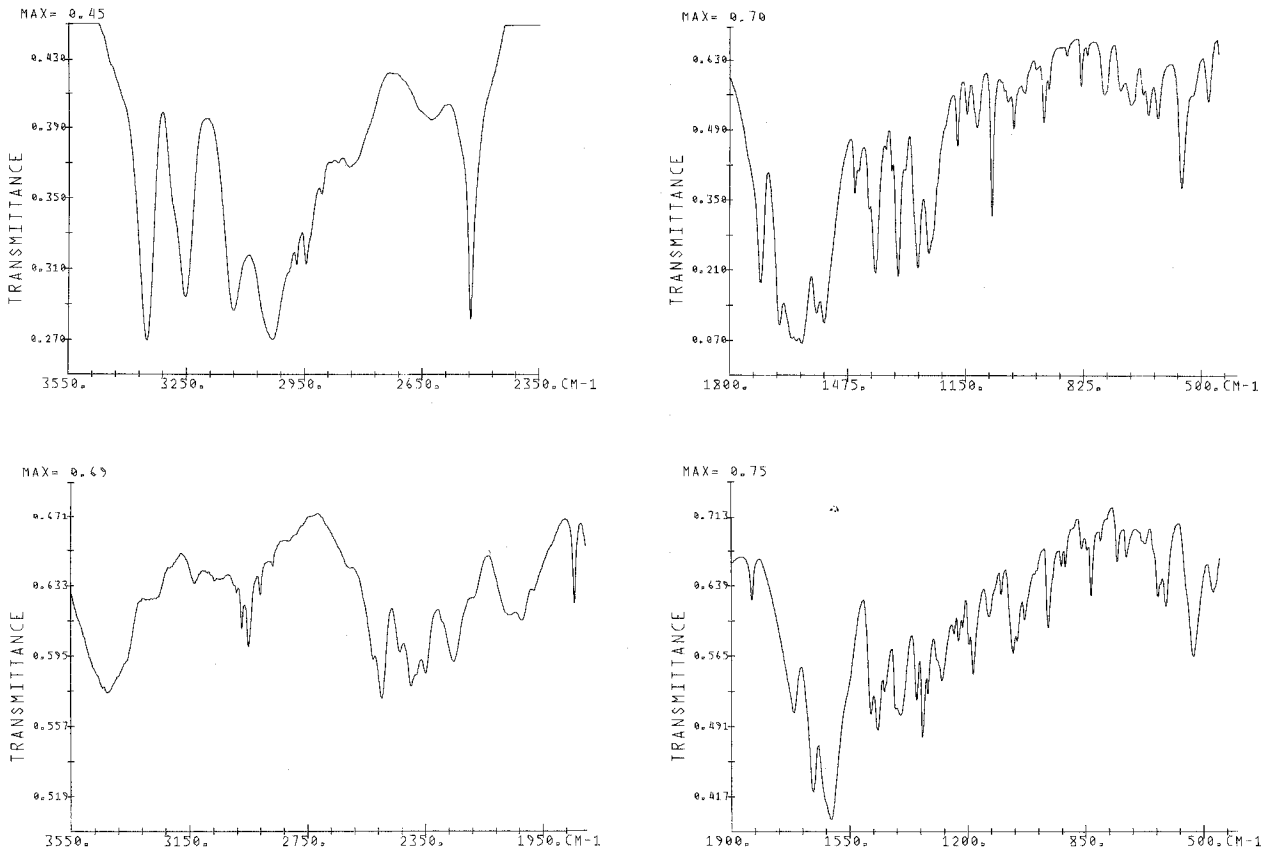

Figure 1. Infrared spectra of (a) crystalline glutathione (upper) and (b) crystalline glutathione—ND, SD, OD (lower).

coordinates of (x, y, z), $(1.5 - x, 1 - y, 0.5 + z)$, $(1 - x, -0.5 + y, 0.5 - z)$, and $(-0.5 + x, 1.5 - y, 1 - z)$. Molecules 2, 3, and 4 are related to molecule 1 by screw rotations about the z axis at $(\frac{3}{4}, \frac{1}{2}, 0)$, about the y axis at $(\frac{1}{2}, 0, \frac{1}{4})$, and about the x axis at $(0, \frac{3}{4}, \frac{1}{2})$, respectively. The unit cell vibrations belong to four symmetry species, A, B_1, B_2, and B_3, the symmetry coordinates of each species being linear combinations of the local symmetry coordinates with coefficients (1, 1, 1, 1), (1, 1, −1, −1), (1, −1, 1, −1), and (1, −1, −1, 1). The A species modes are only Raman active; the B species modes are ir and Raman active.

The structure of an individual molecule, shown in Figure 4, was based on that in the crystal. The dihedral angles were those of the crystal structure, although the peptide groups in the main chain were given standard bond lengths and angles[8] in order to be initially consistent with the empirical force field.[8] For this reason the peptide groups were also kept planar (one dihedral angle deviates significantly from planarity, C7C8N10C11 = −167.0°, while the other is nearly planar, C11C14N16C17 = −176.8°; the assumption of planarity in the former was found to have no significant effect on the normal mode frequencies). The geometry of the NH_3^+ and CO_2^- end groups was the same as before,[9-11] namely N1–H^+ = 1.037 Å, C3–O^- = 1.249 Å, angles about N1 tetrahedral, C2C3O4 = 117.2°, and O4C3O5 = 125.6°. Consistent with the x-ray structure, N1CCO4 = −18.6° and N1CCO5 = 161.5°. The geometries of the Cys and Gly end groups were taken from the ab initio calculations. The crystal structure shows that NCCS = 69.95° and CCSH = 88.65° for the Cys side chain, corresponding to a B conformation[14] ($C^\alpha C^\beta SH \sim 90°$), with geometric parameters of [12] C11C12 = 1.539 Å, CS = 1.832 Å, SH = 1.327 Å, CCS = 112.7°, and CSH = 97.7°. For the Gly structure[13] the parameters are CO19 = 1.200 Å, CO20 = 1.308 Å, O20H = 0.966 Å, CCO19 = 114.4°, and O19CO = 122.6°. The hydrogen-bond system is very complex, all potential groups being involved in the three-dimensional hydrogen-bond network. All of the pendant atoms were included in the normal mode calculation, and the geometric parameters of these hydrogen bonds are given in Table I.

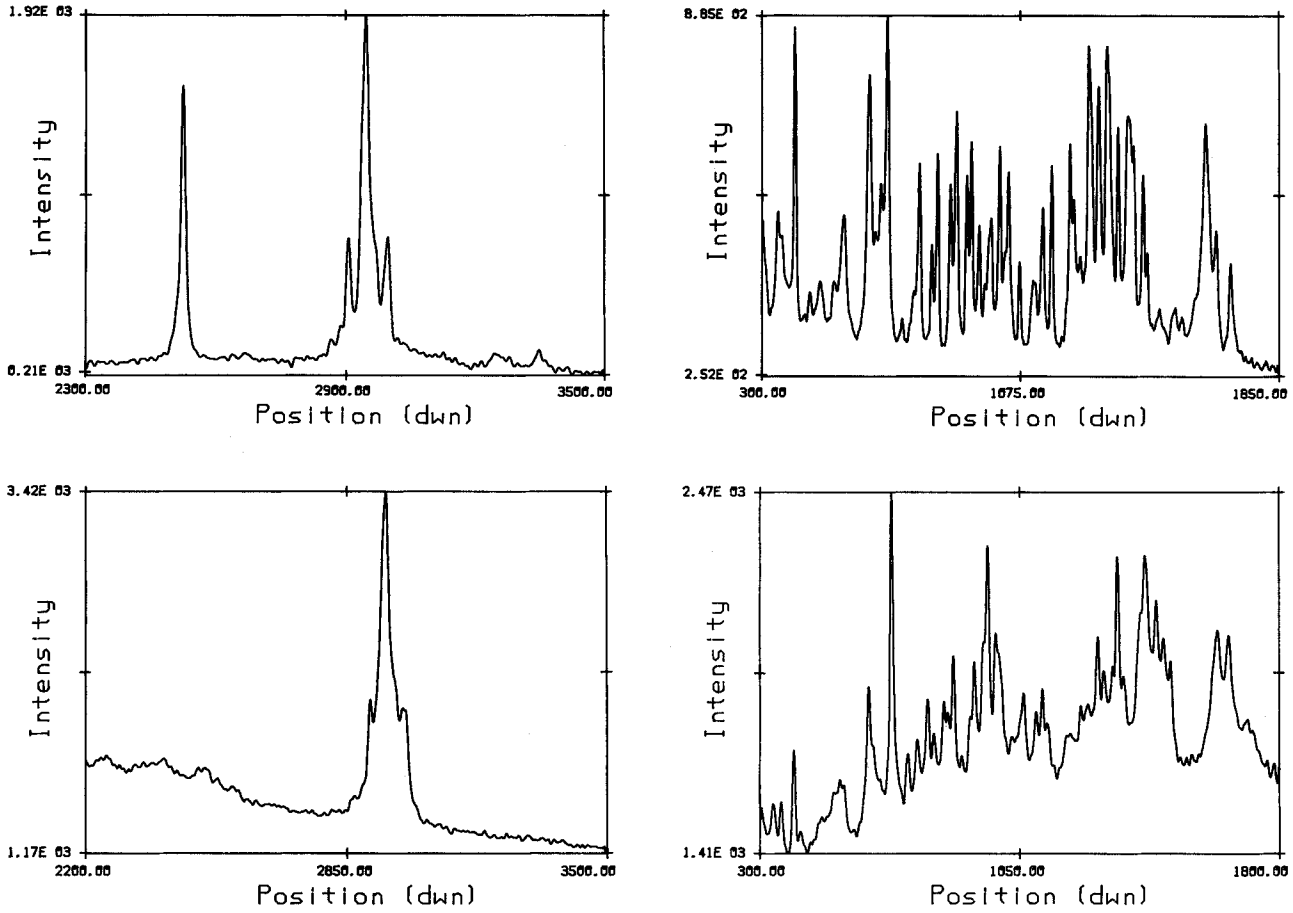

Figure 2. Raman spectra of (a) crystalline glutathione (upper) and (b) crystalline glutathione—ND, SD, OD (lower).

Force Field

The force field used in the GSH normal mode calculation consisted of a combination of force fields for the five components of the structure: empirical force fields for the peptide chain, the NH_3^+ and CO_2^- end groups, and the $C^{\beta}H_2C^{\gamma}H_2$ segment of the Glu residue, and ab initio force fields for the CH_2SH side chain of Cys and the CH_2COOH end group of Gly.

The use of empirical force fields for the peptide chain[8] is determined by the fact that these are the best that are presently available. Nevertheless, they suffer from limitations that must somehow be dealt with. Besides the lack of explicit conformation dependence of the force constants, perhaps the most serious problem is the dependence of certain important force constants, such as N—H stretch (s) C=O s, O···H s, and NH in-plane (ib) and out-of-plane (ob) bends, on the hydrogen-bond strengths. To deal with this problem, we assume that, as clearly confirmed by ab initio calculations,[15] the stretching force constants vary roughly inversely with their respective bond lengths and the bending force constants vary roughly directly with the hydrogen-bond strength. Starting with the empirical values,[8] these force constants were then refined by least-squares fitting in accord with the above principles.

The force constants for the $C7H_2$—C8O and N16H—$C17H_2$ parts of the main chain were taken from those for polyglycine I,[8] while those for the N10H through C14O part of the chain were taken from those for β-poly(L-alanine).[8] The N—H s constants were determined by fitting to the two clearly assignable N—H s bands in the ir spectrum, and their values were consistent with the expectation[15] that the larger force constant should be associated with the shorter N—H bond length, i.e., weaker hydrogen bond (N10H = 0.818 Å, N16H = 0.905 Å). The C=O s constants were determined from their bond lengths (C8O = 1.230 Å, C14O = 1.245 Å) according to a previously observed dependence.[11] The O···H s force constants were ob-

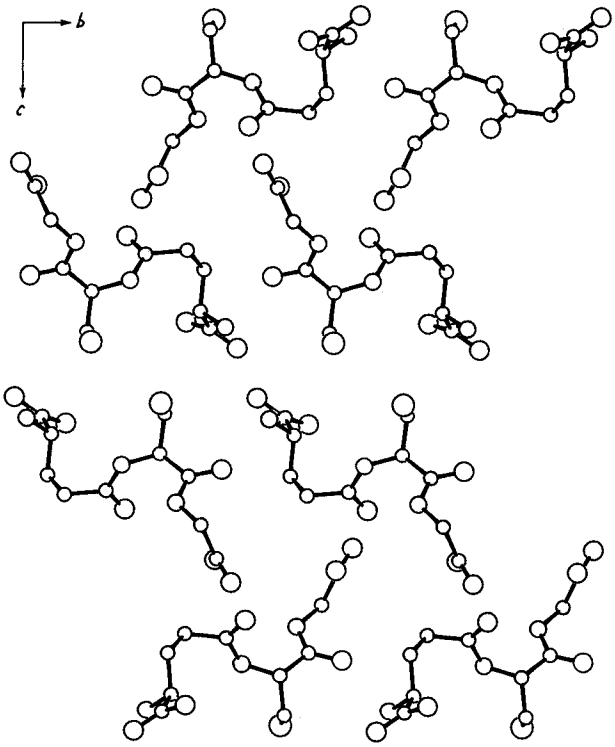

Figure 3. Molecular arrangement in unit cell of glutathione.

Table I Geometric Parameters[a] of Hydrogen Bonds of Glutathione

Hydrogen Bond	H···O O···H	X-H···O C-O···H
N1H1···O4	2.09	151.3
N1H2···O15	1.98	146.0
N1H3···O5	1.96	157.8
N10H···O5	2.14	161.4
N16H···O19	2.10	142.7
O20H···O9	1.84	159.5
S13H···O4	2.34	159.9
C3O4···H1N1	2.09	147.8
C14O15···H2N1	1.98	130.8
C3O5···H3N1	1.96	106.2
C3O5···HN10	2.14	153.8
C18O19···HN16	2.10	138.8
C8O9···HO20	1.84	112.8
C3O4···HS13	2.34	136.1

[a] Lengths in Ångstrom, angles in degrees.

tained from a relationship relating the value of this force constant to d(O···H),[16] which was based on values refined for α- and β-poly(L-alanine).[8] The NH ib force constants were refined to the amide II modes, and resulted in the expected relative values. The NH ob force constant for the Cys residue, which would normally be larger,[8] was given the same value as that for the Gly residue because of its weak hydrogen bond. The values of all these force constants, as well as some others that needed small adjustments, are given in Table II.

Our previous studies of the NH_3^+ and CO_2^- end group modes in the tripeptides[9-11] and β-Ca-poly(L-

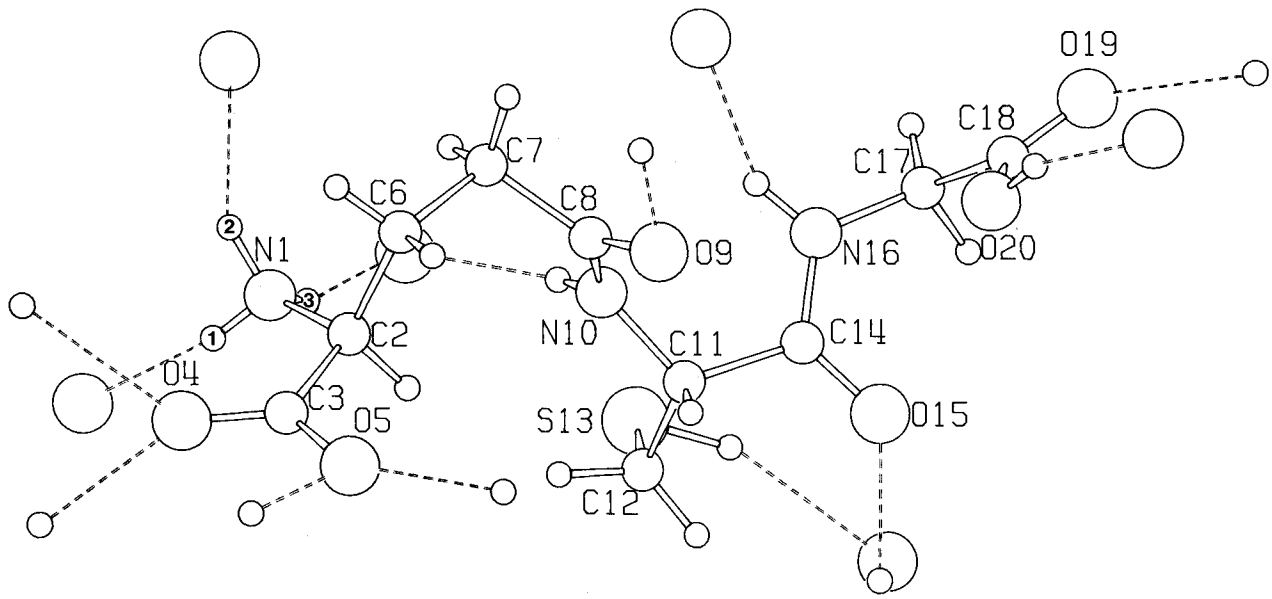

Figure 4. Molecular structure and atom numbering of glutathione, including intermolecular hydrogen bonds (broken lines).

Table II Modified Force Constants for Glutathione Force Field

Group	Force Constant[a]	Value[b]	Group	Force Constant[a]	Scale Factor[c]
Peptide[d]	N10H	6.158	CH_2SH[g]	SH	0.947
	N16H	5.827		CS	0.953
	C8O	9.646		CC	0.944
	C14O	9.222		CCS	0.974
	C8N	6.678		CSH	0.908
	C14N	6.678			
	N10H ob	0.129	CH_2COOH[h]	C18O19	1.0278
	N16H ob	0.129		NC17H	1.0401
	C8O ob	0.530		CCO20	1.1225
	C14O ob	0.560		OCO	0.9337
	N10C11	4.310		COH	0.510
	C11C14	4.700		OH..O	0.2547
	$H^{\alpha}C^{\alpha}C^{\beta}$	0.5486			
	NC2H, C3C2H	0.0324			
	NC11H, C14C11H	0.0525			
CC7C[e]	C2C6	5.126			
	C6C7	4.247			
	C7C8	4.534			
	CC7C	1.240			
	CC6C	1.240			
Hydrogen bonds[f]	N1H1···O4	0.055			
	N1H2···O15	0.079			
	N1H3···O5	0.084			
	N10H···O5	0.042			
	N16H···O19	0.051			
	O20H···O9	0.119			
	SH···O4	0.013			

[a] ob, out-of-plane bend.
[b] Units: mdyn/Å for stretch, mdyn Å for all other constants.
[c] Scale factors to scaled force constants for group; other constants as in pertinent reference.
[d] Other force constatns as in Ref. 8.
[e] Other force constants as in Ref. 17.
[f] From relationship in Ref. 16.
[g] Other force constants as in Ref. 12.
[h] Other force constants as in Ref. 13.

glutamate),[17] as well as studies of others on amino acids,[18] have shown that the force constants for these groups vary somewhat from one molecule to another. This is to be expected since the hydrogen-bonding structures differ between molecules. It is therefore inevitable that some adjustment of these force constants will also be necessary for GSH. To avoid some arbitrariness in the choice of these force constants resulting from the redundancies around the N^+ and C^- atoms, and to make it easier to compare the different force fields, all the force fields available for these end groups were first transformed into a common force field in which, to minimize the number of constants, the following off-diagonal force constants were set equal to zero: CO, $C^{\alpha}CO'$; NC^{α}, $C^{\alpha}NH$; $NC^{\alpha}H$, $C^{\alpha}NH$; HNH, HNH'; $C^{\alpha}NH$,HNH; $C^{\alpha}C$, $C^{\alpha}CO$; and $C^{\alpha}CO$, $C^{\alpha}CO'$. (Conversion of the different force fields in internal coordinates to common force fields in the same local symmetry coordinates of course makes them equivalent for purposes of comparison.[19]) The Val-Gly-Gly force field[9] was used as a starting point, and the force constants were then refined to confidently assignable relevant bands in the GSH spectra. These force constants are given in Table III, where they are compared with comparable values for other molecules. It can be seen that the GSH values are reasonable in relation to those from our previous studies.[9-11,17]

The γ-glutamyl linkage in GSH, rather than being of the typical α-carboxyl type, is unusual and may be partly responsible, together with the close intermolecular C8···O20 contact,[4] for the deviation from planarity of the C8N10 peptide group. The force constants associated with C6 and C7 were

Table III Force Constants[a] for NH_3^+ and CO_2^- End Groups

Force Constant[b]	GSH[c]	VGG[d]	Gly_3[e]	Ala_3(ap)[f]	Ala_3(p)[f]	Ca(Glu)$_n$[g]	Amino Acids[h]
NH_3^+							
NH	5.230	5.163	5.350	5.163	5.163		5.387
NC^α	4.640	4.832	4.500	4.523	4.523		3.890
NC^α t	0.366	0.250	0.200	0.366	0.366		0.049
HNH	0.541	0.564	0.583	0.553	0.554		0.618
$C^\alpha NH$	0.845	0.814	0.777	0.836	0.814		0.734
NH, NH	0.022	0.022	0.022	0.022	0.022		0.018
NC^α, HNH	−0.461	−0.444	−0.444	−0.444	−0.444		−0.307
$C^\alpha NH$, $C^\alpha NH$	−0.085	−0.055	−0.080	−0.080	−0.055		−0.022
CO_2^-							
CO	8.553	9.500	9.500	9.400	9.400	9.310	9.800
$C^\alpha C$	4.116	4.160	4.409	4.160	4.160	4.160	4.390
OCO	1.895	2.000	2.033	2.100	2.000	1.933	1.006
$C^\alpha CO$	1.299	1.209	1.109	0.511	0.611	1.209	1.430
CO_2 w	0.746	0.577	0.636	0.542	0.542	0.542	0.607
CO, CO	0.421	1.400	1.200	1.300	1.400	1.300	1.300
CO, $C^\alpha C$	0.483	0.958	1.439	0.958	0.958	1.439	0.000
CO, OCO	0.352	0.374	0.374	0.509	0.509	0.374	2.180
CO, $C^\alpha CO$	0.842	1.209	1.018	1.398	1.398	1.018	1.289
$C^\alpha C$, OCO	−0.945	−0.952	0.519	−0.847	−0.847	−0.652	−0.392
CO_2 w, OCO	0.0	0.0	0.0	0.0	0.0	0.0	0.044

[a] Units: mydn/Å for stretch and stretch, stretch constants; mdyn for stretch, bend constants; mdyn Å for all others.
[b] t, Torsion; w, wag.
[c] Glutathione, this work.
[d] Valyl-glycyl-glycine, Ref. 9.
[e] Triglycine, Ref. 10.
[f] Trialanine, Ref. 11. ap, antiparallel chain; p, parallel chain.
[g] β-Ca-poly(L-glutamate), Ref. 17.
[h] Amino acids: cysteine, serine, β-chloroalanine, Ref. 18.

therefore first transferred from β-Ca-poly(L-glutamate),[18] and then some adjustments were made since the linkage of C7 to the peptide group makes it somewhat similar to the C^α of Gly. These modified force constants are given in Table II.

In the case of the CH_2SH group, we have a conformation-dependent ab initio force field[12] that can be transferred to GSH. As noted, this group in GSH has a conformation with $C^\alpha C^\beta SH \sim 90°$, and we have therefore used an ab initio force field that is the mean of the *gauche* (60°) and skew (120°) force constants.[12] These and the empirical constants in the adjoining chain were merged as previously.[12] Some small changes were then made to give better agreement with bands clearly assignable to this moiety, and the modified scale factors for these force constants are given in Table II.

The force field for the CH_2COOH group was obtained from an ab initio calculation of a model system consisting of a glycine molecule, in a conformation similar to that found in GSH, with two water molecules hydrogen bonded to the COOH group.[13] The motivation for this approach was to try to define the C—O s and COH bend (b) modes with greater confidence than would be possible by using empirical force fields for the acid group. These coordinates contribute to many modes, and their sensitivity to the hydrogen-bond structure makes their assignment in the spectrum far from obvious. By comparing the results for the hydrogen bonded with those for the isolated glycine,[13] it seems possible to arrive at reasonable initial values of the relevant force constants that can then be readily refined from the observed bands. Several aspects of this procedure are worth noting. First, the COH b force constant is much more sensitive to hydrogen bonding than C=O s or C—O s: the ratio of hydrogen-bonded to isolated values is 1.84, 0.91, and 1.15, respectively. It might be expected, therefore, that COH b would be quite sensitive to variations in hydrogen-bond

structure. Second, the shifts in the C=O s and C—O s frequencies between COOH and COOD are very sensitive to the COH b components of these modes, and therefore to the COH b force constant. From GSH to GSD, C=O s does not shift and C—O s shifts down by ~3 cm^{-1}. This behavior can only be reproduced by a much smaller COH b force constant than in the glycine model, which we attribute to the very different hydrogen-bond structures: for example, besides the qualitative difference between the O20H···O (water) and O20H···O9C8 bonds, the C18O20H···O9 dihedral angles are very different, −1.1° vs −120.5°, respectively. Finally, because of the latter angle difference, the important COH, OH···O interaction force constant must change sign, since the definition of the OH···O internal coordinate involves a sign reversal between 0° and 180°. The scale factors for these modified force constants are given in Table II.

Transition dipole coupling,[20,21] in the dipole derivative coupling (DDC) formalism,[9] was computed for the amide I and amide II modes. Since the respective force constants for the two peptide groups are different (because of the different hydrogen bond structures), the intramolecular modes are relatively pure and this interaction effect is very small. Because of the large distances between equivalent groups in the unit cell, the calculated shifts for different symmetry species are also very small.

RESULTS AND DISCUSSION

The internal and local symmetry coordinates of the hydrogen-bonded GSH are given in Tables IV and V, respectively. The observed ir and Raman bands and the calculated normal modes and potential energy distributions (PED) of GSH are given in Table VI, and the comparable quantities for GSD are given in Table VII. We present results only in the region of observation, above about 300 cm^{-1}. Below this region, the modes involve low frequency skeletal deformations and intermolecular hydrogen-bond motions. Since these force constants are at best uncertain, and nonbonded interactions between molecules have not been included in the calculation, it is not fruitful at this stage to place much confidence in the details of this low frequency region.

Most of the assignments, which are based on the deuteration results and the normal mode calculations, are generally quite satisfactory. Spectra of other isotopic derivatives would obviously be valuable in confirming those that are less certain.

XH Stretch Region

A detailed assignment of the NH s modes is complicated by the Fermi resonances in this region[22] and the overlap with the OH s and NH_3^+ s modes. Nevertheless, reasonable assignments can be suggested. For the latter group, consistent with results on other tripeptides,[9-11] we assign NH_3^+ symmetric stretch (ss), calculated at 3027 cm^{-1}, to the observed band at 3031 cm^{-1}, probably overlapped with amide B (found at 3058–3080 cm^{-1} in polypeptides[22]); and we assign NH_3^+ antisymmetric stretch (as), calculated at 3122 and 3111 cm^{-1}, to the observed band at 3130 cm^{-1}. If the 3251 cm^{-1} band is assigned to NH_3^+ as, then there are no reasonable assignments for the 2396 and 2346 cm^{-1} bands of GSD. With our proposed assignments, the observed GSD bands at 2346 and 2189 cm^{-1} are accounted for (making allowances for differences in anharmonicities between NH and ND modes) by calculated NH_3^+ as and ND_3^+ ss modes at 2316, 2310, and 2174 cm^{-1}, respectively. (We attribute the relatively strong 2252 cm^{-1} band, as well as comparable bands at 2061 and 2018 cm^{-1}, to combinations and/or overtones.) The N16H s and N10H s modes are then naturally assigned to calculated (and observed) bands at 3262 (3251) and 3344 (3348) cm^{-1}, respectively. Their shift to 2403 (2396) and 2462 (2495) cm^{-1}, respectively, in GSD supports this assignment.

Since the N16H···O is the stronger of the two peptide hydrogen bonds, the N16H s band would be expected to be the more intense.[23] This is not the case, suggesting that the observed 3348 cm^{-1} band may contain another contribution. (Part of its intensity may be due to what seems to be a broad underlying band centered near 3425 cm^{-1}—compare the GSD spectrum—and perhaps due to water on the KBr pellet.) We assign the OH s mode also to this band for two main reasons: in the glycine-$(H_2O)_2$ model[13] this frequency occurs near 3340 cm^{-1}, and in GSD the OD s mode separates from N10D s, being predicted at 2443 cm^{-1} with a band being observed at 2434 cm^{-1}.

Seven observed ir and Raman bands in the 3000–2850 cm^{-1} region that remain unchanged from GSH to GSD can be assigned to CH_2 and CH stretch modes. (The 2834 cm^{-1} band of GSH is much weaker in GSD, and is probably a combination band.) Fermi resonances are also involved in this region,[24] but preliminary reasonable assignments seem possible. The $C12H_2$ as mode at 2979 (2970) cm^{-1} and the $C12H_2$ ss mode at 2937 (2935) cm^{-1} are consistent with similar bands found in ethanethiol at 2980 and

Table IV Internal Coordinates of GSH

Bonds

R1 = Δr(N1–C2)	R16 = Δr(C8–O9)	R31 = Δr(C12–H1)
R2 = Δr(N10–C11)	R17 = Δr(C14–O15)	R32 = Δr(C12–H2)
R3 = Δr(N16–C17)	R18 = Δr(C18–O19)	R33 = Δr(C12–S13)
R4 = Δr(C2–C3)	R19 = Δr(C2–C6)	R34 = Δr(S13–H)
R5 = Δr(C11–C14)	R20 = Δr(C6–C7)	R35 = Δr(C18–O20)
R6 = Δr(C17–C18)	R21 = Δr(C11–C12)	R36 = Δr(O20–H)
R7 = Δr(C8–N10)	R22 = Δr(C7–C8)	R37 = Δr(O4···H1[N1])
R8 = Δr(C14–N16)	R23 = Δr(C2–H)	R38 = Δr(O4···H[S])
R9 = Δr(N1–H1)	R24 = Δr(C11–H)	R39 = Δr(O5···H3[N1])
R10 = Δr(N1–H2)	R25 = Δr(C17–H1)	R40 = Δr(O5···H[N10])
R11 = Δr(N1–H3)	R26 = Δr(C17–H2)	R41 = Δr(O9···H)
R12 = Δr(N10–H)	R27 = Δr(C6–H1)	R42 = Δr(O15···H)
R13 = Δr(N16–H)	R28 = Δr(C6–H2)	R43 = Δr(O19···H)
R14 = Δr(C3–O4)	R29 = Δr(C7–H1)	
R15 = Δr(C3–O5)	R30 = Δr(C7–H2)	

Angles

R44 = $\Delta\theta$(H1–N1–H2)	R70 = $\Delta\theta$(C7–C6–H1)	R96 = $\Delta\theta$(C12–S–H)
R45 = $\Delta\theta$(H2–N1–H3)	R71 = $\Delta\theta$(C6–C7–C8)	R97 = $\Delta\theta$(C11–C14–N16)
R46 = $\Delta\theta$(H1–N1–H3)	R72 = $\Delta\theta$(C8–C7–H2)	R98 = $\Delta\theta$(N16–C14–O15)
R47 = $\Delta\theta$(C2–N1–H1)	R73 = $\Delta\theta$(H1–C7–H2)	R99 = $\Delta\theta$(C11–C14–O15)
R48 = $\Delta\theta$(C2–N1–H2)	R74 = $\Delta\theta$(C6–C7–H1)	R100 = $\Delta\theta$(C14–O15···H)
R49 = $\Delta\theta$(C2–N1–H3)	R75 = $\Delta\theta$(C6–C7–H2)	R101 = $\Delta\theta$(C14–N16–C17)
R50 = $\Delta\theta$(N1–C2–C3)	R76 = $\Delta\theta$(C8–C7–H1)	R102 = $\Delta\theta$(C14–N16–H)
R51 = $\Delta\theta$(N1–C2–C6)	R77 = $\Delta\theta$(C7–C8–N10)	R103 = $\Delta\theta$(C17–N16–H)
R52 = $\Delta\theta$(C3–C2–C6)	R78 = $\Delta\theta$(N10–C8–O9)	R104 = $\Delta\theta$(N16–C17–C18)
R53 = $\Delta\theta$(H–C2–C6)	R79 = $\Delta\theta$(C7–C8–O9)	R105 = $\Delta\theta$(C18–C17–H2)
R54 = $\Delta\theta$(N1–C2–H)	R80 = $\Delta\theta$(C8–O9···H)	R106 = $\Delta\theta$(H1–C17–H2)
R55 = $\Delta\theta$(H–C2–C3)	R81 = $\Delta\theta$(C8–N10–C11)	R107 = $\Delta\theta$(N16–C17–H1)
R56 = $\Delta\theta$(O4–C3–O5)	R82 = $\Delta\theta$(C8–N10–H)	R108 = $\Delta\theta$(N16–C17–H2)
R57 = $\Delta\theta$(C2–C3–O4)	R83 = $\Delta\theta$(C11–N10–H)	R109 = $\Delta\theta$(C18–C17–H1)

2931 cm^{-1}, respectively.[12] Expected $C^{\alpha}H^{\alpha}$ modes are well predicted near the observed band at 2863 cm^{-1}. The $C17H_2$ modes correspond to similar bands found for such a terminal group in other tripeptides,[9,10] and the $C6H_2$, $C7H_2$ modes are also fairly well accounted for. Secure assignments in this region will clearly be possible only when CD_2-substituted molecules can be studied.

The SH s mode is confidently assignable to the observed 2524 cm^{-1} band of GSH. However, its frequency is much lower than the 2560–2565 cm^{-1} found for ethanethiol in the condensed state.[12] Part of this difference may be due to differences in the nature of the hydrogen bonding, since conformational differences do not significantly affect this mode.[12] Another possibility is a Fermi resonance interaction with a combination band (for example, a possibility involving this group is 1559 + 1015 = 2574), giving rise to the observed 2625 and 2524 cm^{-1} bands. The shift to 1837 cm^{-1} in GSD confirms this general assignment, although this band may also be involved in Fermi resonance with the 1865 cm^{-1} band.

Amides I and II Region

This region, from 1720–1490 cm^{-1}, can be very well assigned, despite the overlap from bands due to the NH_3^+ and CO_2^- groups.

The ir band at 1713 cm^{-1} is clearly due to CO19 s, being calculated at 1711 cm^{-1} with the comparable force constant transferred without change from the ab initio glycine model force field.[13] As noted above, the absence of a shift in GSD is due to a very small contribution of COH b to this mode, which helps to determine the latter force constant.

The two amide I modes (mainly C=O s with some CN s) are well predicted, based on their C=O bond lengths and respective force constants (the CO19 bond length of 1.195 Å and its higher frequency fits in with this general relationship). The unperturbed modes were calculated at 1660.1 cm^{-1}

Table IV (*Continued*)

Angles

R58 = Δθ(C2–C3–O5)	R84 = Δθ(N10–C11–C14)	R110 = Δθ(C17–C18–O20)
R59 = Δθ(H1···O4···H[S])	R85 = Δθ(N10–C11–C12)	R111 = Δθ(O19–C18–O20)
R60 = Δθ(C3–O4···H1)	R86 = Δθ(C14–C11–C12)	R112 = Δθ(C17–C18–O19)
R61 = Δθ(C3–O4···H[S])	R87 = Δθ(C12–C11–H)	R113 = Δθ(C18–O19···H)
R62 = Δθ(H3···O5···H[N10])	R88 = Δθ(N10–C11–H)	R114 = Δθ(C18–O20–H)
R63 = Δθ(C3–O5···H3)	R89 = Δθ(C14–C11–H)	R115 = Δθ(N1–H3···O)
R64 = Δθ(C3–O5···H[N10])	R90 = Δθ(C11–C12–S)	R116 = Δθ(N1–H2···O)
R65 = Δθ(C2–C6–C7)	R91 = Δθ(S–C12–H2)	R117 = Δθ(N1–H1···O)
R66 = Δθ(C7–C6–H2)	R92 = Δθ(H1–C12–H2)	R118 = Δθ(N10–H···O)
R67 = Δθ(H1–C6–H2)	R93 = Δθ(C11–C12–H1)	R119 = Δθ(S–H···O)
R68 = Δθ(C2–C6–H1)	R94 = Δθ(C11–C12–H2)	R120 = Δθ(N16–H···O)
R69 = Δθ(C2–C6–H2)	R95 = Δθ(S–C12–H1)	R121 = Δθ(O20–H···O)

Out of Plane Angles

R122 = Δφ(C8–O9–C7–N10)	R126 = Δφ(N16–H–C14–C17)
R123 = Δφ(C14–O15–C11–N16)	R127 = Δφ(C3–C2–O4–O5)
R124 = Δφ(C18–O19–O20–C17)	R128 = Δφ(O4-C3–H1–H[S])
R125 = Δφ(N10–H–C8–C11)	R129 = Δφ(O5–C3–H3–H[N10])

Torsions

R130 = Δτ(N1–C2)	R143 = Δτ(C3–O4)
R131 = Δτ(N10–C11)	R144 = Δτ(C3–O5)
R132 = Δτ(N16–C17)	R145 = Δτ(C8–O9)
R133 = Δτ(C2–C3)	R146 = Δτ(C14–O15)
R134 = Δτ(C11–C14)	R147 = Δτ(C18–O19)
R135 = Δτ(C17–C18)	R148 = Δτ(C2–C6)
R136 = Δτ(C8–N10)	R149 = Δτ(C6–C7)
R137 = Δτ(C14–N16)	R150 = Δτ(C11–C12)
R138 = Δτ(N1–H1)	R151 = Δτ(C7–C8)
R139 = Δτ(N1–H2)	R152 = Δτ(C12–S)
R140 = Δτ(N1–H3)	R153 = Δτ(S–H)
R141 = Δτ(N10–H)	R154 = Δτ(C18–O20)
R142 = Δτ(N16–H)	R155 = Δτ(O20–H)

for amide I of C8N, with DDC shifts of 0.5 (A), −4.2 (B_1), 0.5 (B_2), and 1.7 (B_3) cm^{-1}, and at 1627.2 cm^{-1} for amide I of C14N, with DDC shifts of 0.6 (A), 2.1 (B_1), 1.9 (B_2), and 1.2 (B_3) cm^{-1}. The small shifts are of course due to the very different unperturbed frequencies, and consequent minimal mixing of the two modes in the eigenvectors of one molecule, and the relatively large separation of equivalent groups between the four molecules in the unit cell. The observed downshifts on deuteration, about 6 and 10 cm^{-1}, respectively, are moderately well reproduced, viz., 5 and 6 cm^{-1}, respectively.

The NH_3^+ ab mode can be assigned to the 1615 cm^{-1} band, which disappears on deuteration, and the similar behavior of the 1492 cm^{-1} band suggests its assignment to NH_3^+ sb. Both of these are well reproduced by the calculation, 1618 and 1492 cm^{-1}, respectively. The other component of NH_3^+ ab, predicted at 1595 cm^{-1}, may be within the 1600 cm^{-1} band, which, because it is not much affected by deuteration, we assign to CO_2^- as. ND_3^+ as modes are predicted at 1155 and 1116 cm^{-1}, with the new 1117 cm^{-1} band being assignable to the latter. The new bands at 1098 and 1063 cm^{-1} in GSD can be assigned to ND_3^+ sb, predicted at 1090 and 1066 cm^{-1}, respectively.

The amide II modes (NH ib + CN s) are well assigned to the two bands at 1559 and 1537 cm^{-1}, with the higher frequency band associated with the more strongly hydrogen bonded group, N16H. These modes are predicted to shift on deuteration to 1492 (C14N s) and 1471 (mostly $C7H_2$ b but with a significant C8N s component) cm^{-1}, and new bands are observed in GSD at 1486 and 1465 cm^{-1}. The DDC contributions to amide II are very small (<0.5 cm^{-1}).

Table V Local Symmetry Coordinates of GSH

Symmetry Coordinate	Description[a]	Symmetry Coordinate	Description[a]
	Stretches		
S1 = R1	N1C s	S23 = R23	C2H s
S2 = R2	NC11 s	S24 = R24	C11H s
S3 = R3	NC17 s	S25 = R25 + R26	$C17H_2$ ss
S4 = R4	CC3 s	S26 = R25–R26	$C17H_2$ as
S5 = R5	CC14 s	S27 = R27 + R28	$C6H_2$ ss
S6 = R6	C17C s	S28 = R27–R28	$C6H_2$ as
S7 = R7	C8N s	S29 = R29 + R30	$C7H_2$ ss
S8 = R8	C14N s	S30 = R29–R30	$C7H_2$ as
S9 = R9 + R10 + R11	NH_3 ss	S31 = R31 + R32	$C12H_2$ ss
S10 = R9–R10	NH_3 as1	S32 = R31–R32	$C12H_2$ as
S11 = 2R11–R9–R10	NH_3 as2	S33 = R33	CS s
S12 = R12	N10H s	S34 = R34	SH s
S13 = R13	N16H s	S35 = R35	CO20 s
S14 = R14 + R15	CO_2 ss	S36 = R36	OH s
S15 = R14–R15	CO_2 as	S37 = R37	O4···H1[N1] s
S16 = R16	C8O s	S38 = R38	O4···H[S] s
S17 = R17	C14O s	S39 = R39	O5···H3[N1] s
S18 = R18	CO19 s	S40 = R40	O5···H[N10] s
S19 = R19	C2C6 s	S41 = R41	O9···H s
S20 = R20	C6C7 s	S42 = R42	O15···H s
S21 = R21	CC12 s	S43 = R43	O19···H s
S22 = R22	CC8 s		
	Deformations		
S44 = R44 + R45 + R46–R47–R48–R49	NH_3 sb	S76 = 2R84–R85–R86	C12 b1
S45 = 2R44–R45–R46	NH_3 ab1	S77 = R85–R86	C12 b2
S46 = R45–R46	NH_3 ab2	S78 = 2R87–R88–R89	H^{α}[C11] b1
S47 = 2R47–R48–R49	NH_3 r1	S79 = R88–R89	H^{α}[C11] b2
S48 = R48–R49	NH_3 r2	S80 = 5R90–R91–R92–R93–R94–R95	CCS d
S49 = R50 + R51 + R52–R53–R54–R55	NCC3 d	S81 = 4R92–R91–R93–R94–R95	$C12H_2$ b
S50 = 2R50–R51–R52	C3 b1	S82 = R91–R93–R94 + R95	$C12H_2$ w
S51 = R51–R52	C3 b2	S83 = −R91 + R93–R94 + R95	$C12H_2$ r
S52 = 2R53–R54–R55	H^{α}[C2] b1	S84 = R91 + R93–R94–R95	$C12H_2$ tw
S53 = R54–R55	H^{α}[C2] b2	S85 = R96	CSH b
S54 = 2R56–R57–R58	CO_2 b	S86 = 2R97–R98–R99	CC14N d
S55 = R57–R58	CO_2 r	S87 = R98–R99	C14O ib
S56 = 2R59–R60–R61	O4···H_2 b	S88 = R100	C14O···H b
S57 = R60–R61	O4···H_2 r	S89 = 2R101–R102–R103	CN16C d
S58 = 2R62–R63–R64	O5···H_2 b	S90 = R102–R103	N16H ib
S59 = R63–R64	O5···H_2r	S91 = 5R104–R105–R106–R107–R108–R109	NC17C d
S60 = 5R65–R66–R67–R68–R69–R70	CC6C d	S92 = 4R106–R105–R107–R108–R109	$C17H_2$ b
S61 = 4R67–R66–R68–R69–R70	$C6H_2$b	S93 = R105–R107–R108 + R109	$C17H_2$ w
S62 = R66–R68–R69 + R70	$C6H_2$ w	S94 = −R105 + R107–R108 + R109	$C17H_2$ r
S63 = −R66 + R68–R69 + R70	$C6H_2$ r	S95 = R105 + R107–R108–R109	$C17H_2$ tw

1500–1100 cm^{-1} Region

The region from 1500 to about 1100 cm^{-1} usually encompasses a number of CH_2 and CH as well as NH deformation modes, the CO_2^- ss mode, and the so-called amide III mode. In the case of GSH we also have to include the C—O s and COH b modes. The amide III mode has classically been considered to be a localized NH ib + CN s counterpart to amide II,[25] but as has been pointed out,[8] this is a much oversimplified description. Even in polypeptides CN s may not be a significant contributor, and in small peptides[9-11] it is often absent, with NH ib contributing to many modes in this region. This also seems to be the case for GSH.

The observed bands at 1453 and 1442 cm^{-1} in GSH, which shift to 1445 and 1439 cm^{-1} GSD, are clearly assignable to CH_2 b. Although their frequen-

Table V (*Continued*)

Symmetry Coordinate	Description[a]	Symmetry Coordinate	Description[a]
	Deformations		
S64 = R66 + R68–R69–R70	$C6H_2$ tw	S96 = 2R110–R111–R112	CCO20 d
S65 = 5R71–R72–R73–R74–R75–R76	CC7C d	S97 = R111–R112	C18O ib
S66 = 4R73–R72–R74–R75–R76	$C7H_2$ b	S98 = R113	C18O···H b
S67 = R72–R74–R75 + R76	$C7H_2$ w	S99 = R114	COH b
S68 = −R72 + R74–R75 + R76	$C7H_2$ r	S100 = R115	N1H3···O b
S69 = R72 + R74–R75–R76	$C7H_2$ tw	S101 = R116	N1H2···O b
S70 = 2R77–R78–R79	CC8N d	S102 = R117	N1H1···O b
S71 = R78–R79	C8O ib	S103 = R118	N10H···O b
S72 = R80	C8O···H b	S104 = R119	SH···O b
S73 = 2R81–R82–R83	CN10C d	S105 = R120	N16H···O b
S74 = R82–R83	N10H ib	S106 = R121	O20H···O b
S75 = R84 + R85 + R86–R87–R88–R89	NCC14 d		
	Out-of-plane bends		
S107 = R122	C8O ob	S111 = R126	N16H ob
S108 = R123	C14O ob	S112 = R127	CO_2 w
S109 = R124	CO19 ob	S113 = R128	O4···H_2 w
S110 = R125	N10H ob	S114 = R129	O5···H_2 w
	Torsions		
S115 = R130	N1C t	S128 = R143	CO4 t
S116 = R131	NC11 t	S129 = R144	CO5 t
S117 = R132	NC17 t	S130 = R145	C8O t
S118 = R133	CC3 t	S131 = R146	C14O t
S119 = R134	CC14 t	S132 = R147	CO19 t
S120 = R135	C17C t	S133 = R148	C2C6 t
S121 = R136	C8N t	S134 = R149	C6C7 t
S122 = R137	C14N t	S135 = R150	CC12 t
S123 = R138	N1H1 t	S136 = R151	CC8 t
S124 = R139	N1H2 t	S137 = R152	CS t
S125 = R140	N1H3 t	S138 = R153	SH t
S126 = R141	N10H	S139 = R154	CO20 t
S127 = R142	N16H t	S140 = R155	OH t

[a] s, Stretch; ss, symmetric stretch; as, antisymmetric stretch; b, bend; sb, symmetric bend; ab, antisymmetric bend; ib, in-plane bend; ob, out-of-plane bend; d, deformation; w, wag; tw, twist; r, rock; t, torsion.

cies are generally reproduced, specific assignments must await more detailed information beyond the present assumption of equal HCH b force constants.

The CO_2^- ss mode, calculated at 1395 cm^{-1} with a contribution at 1404 cm^{-1}, is clearly assignable to the strong band at 1396 cm^{-1}, the mixed mode with $C6H_2$ wag (w) being assignable to the weak band at 1413 cm^{-1}. These mode compositions are reversed in GSD, at 1401 (1412) and 1393 (1398) cm^{-1}, and it is interesting to see that the observed relative intensities follow this pattern, in fact being reversed in the Raman.

The C—O s and COH b modes could be expected to fall in this region, based on the analysis of glycine.[13] However, as we noted above, the COH b force constant had to be reduced significantly in order to explain the absence of a shift of the CO19 s frequency in GSD. We expect, therefore, that it will mainly be C—O s that contributes in this region. For the isolated glycine molecule, observed bands at 1253, 1131, and 1101 cm^{-1} contain C—O s contributions.[13] For the glycine conformation found in GSH, these modes are calculated at 1308, 1156, and 844 cm^{-1} for the isolated molecule and at 1363, 1226, and 850 cm^{-1} for the molecule with two water molecules hydrogen bonded to it.[13] Using the C—O s force constant from the latter system, we calculate a main CO20 s mode at ~1337 cm^{-1}, to which strong ir and Raman bands at ~1335 cm^{-1} can be assigned, and a small contribution to a calculated 1368 cm^{-1} $C17H_2$ w mode, to which a strong Raman band at 1368 cm^{-1} can be assigned. Another major CO20 s

Table VI Observed and Calculated Frequencies (in cm^{-1}) of GSH

Observed[a]		Calculated				
Raman	IR	A	B_1	B_2	B_3	Potential Energy Distribution[b]
	3348 m	3346	3346	3346	3346	OH s(108)
		3344	3344	3344	3344	N10H s(99)
	3251 m	3262	3262	3262	3262	N16H s(99)
	3130 m	3122	3122	3122	3122	NH_3 as1(81) NH_3 as2(17)
		3111	3111	3111	3111	NH_3 as2(81) NH_3 as1(18)
	3031 m	3027	3027	3027	3027	NH_3 ss(98)
		3022	3022	3022	3022	$C17H_2$ as(77) $C17H_2$ ss(22)
2997 m		2995	2995	2995	2995	$C7H_2$ as(61) $C6H_2$ as(38)
2989 sh	2990 sh	2992	2992	2992	2992	$C6H_2$ as(61) $C7H_2$ as(38)
	2969 w	2979	2979	2979	2979	$C12H_2$ as(100)
2948 vs	2945 mw	2953	2953	2953	2953	$C17H_2$ ss(78) $C17H_2$ as(24)
	2935 sh	2937	2937	2937	2937	$C12H_2$ ss(100)
2907 m	2906 w	2928	2928	2928	2928	$C6H_2$ ss(71) $C7H_2$ ss(28)
		2925	2925	2925	2925	$C7H_2$ ss(71) $C6H_2$ ss(28)
	2863 w	2866	2866	2866	2866	C2H s(99)
		2864	2864	2864	2864	C11H s(99)
2525 s	2625 w 2524 m	2531	2531	2531	2531	SH s(100)
1706 m	1713 s	1711	1713	1711	1713	CO19 s(92) CCO20 d(10)
1661 m	1661 s	1661	1656	1661	1662	C8O s(71) C8N s(24) CC8N d(10)
1630 s	1627 vs	1628	1629	1628	1628	C14O s(72) C14N s(23)
	1615 m	1618	1619	1619	1618	NH_3 ab2(59) NH_3 r1(21) NH_3 ab1(10)
1597 sh	1600 vs	1603	1601	1601	1603	CO_2 as(99) CO_2 r(11)
		1595	1595	1595	1595	NH_3 ab1(63) NH_3 r2(22) NH_3 ab2(10)
1560 w	1559 ms	1556	1555	1556	1556	N16H ib(47) C14N s(24) CC14 s(14) C14O ib(12)
1541 w	1537 s	1542	1542	1542	1543	N10H ib(53) C8N s(19) CC8 s(11)
1492 w		1494	1495	1495	1494	NH_3 sb(84)
		1451	1451	1451	1451	$C6H_2$ b(63)
1456 w	1453 m	1444	1444	1444	1444	$C12H_2$ b(91)
1443 ms	1442 w	1442	1442	1442	1442	$C17H_2$ b(87)
		1436	1436	1436	1436	$C7H_2$ b(82)
1414w	1413 w	1404	1404	1404	1404	$C6H_2$ w(21) $C6H_2$ b(16) CO_2 ss(16) CC3 s(16)
1397 s	1396 s	1395	1396	1396	1395	CO_2 ss(45) CO_2 b(24) $C6H_2$ tw(12) CC3 s(10)
1368 s	1367 w	1367	1369	1367	1369	$C17H_2$ w(34) C17C s(14) CO20 s(11) $C17H_2$ b(10) CC14 s(10)
1342 sh	1351 w	1354	1355	1354	1355	$C7H_2$ w(28) $C6H_2$ tw(17) CC8 s(13)
1342 sh		1342	1342	1341	1342	H^{α}[C2] b2(32) NH_3 r1(13) $C6H_2$ w(10)
1336 s	1333 s		1339		1339	CO20 s(21) N16H ib(14) C17C s(10)
		1334		1334		CO20 s(35) CO19 ib(16) C17C s(15) N16H ib(13)
1310 s	1314 w	1321		1321		$C17H_2$ w(43) H^{α}[C11] b2(15) N16H ib(14)
			1314		1314	$C17H_2$ w(35) H^{α}[C11] b2(21) CO20 s(13) N16H ib(7)
	1290 sh	1300	1299	1300	1299	$C6H_2$ tw(12) H^{α}[C11] b2(10)
		1291	1290	1291	1291	NH_3 r2(34)
1281 s	1279 s	1275	1275	1275	1275	$C17H_2$ tw(50) H^{α}[C11] b2(11)
1255 w		1260	1260	1260	1260	$C12H_2$ w(48) H^{α}[C11] b1(21) $C12H_2$ tw(11)
	1249 s	1254	1254	1254	1254	H^{α}[C11] b2(29) $C17H_2$ tw(25) N16H ib(12)
		1252	1252	1252	1252	$C7H_2$ w(23) $C7H_2$ tw(22) H^{α}[C2]b1 (21) $C6H_2$ tw(10)
1235 w	1238 sh	1240	1241	1241	1240	NH_3 r1(37) H^{α}[C2] b2(32)
1224 ms	1223 sh	1217	1216	1217	1217	$C6H_2$ tw(23) $C12H_2$ tw(13) $C7H_2$ tw(12)
1200 vw	1203 sh	1201	1201	1201	1201	$C12H_2$ tw(25) $C7H_2$ w(12)
1170 ms	1169 m	1174	1174	1174	1174	H^{α}[C11] b1(43) $C12H_2$ w(27) NC17 s(15)
1143 m	1143 mw	1149	1149	1149	1149	H^{α}[C2] b1(35) $C7H_2$ tw(23) $C6H_2$ w(20) C6C7 s(11)
1121 sh	1123 sh	1125	1125	1125	1125	H^{α}[C11] b1(15) $C12H_2$ tw(13) CC12 s(13) $C12H_2$ tw(13) NC11 s(10)
1115 m	1115 m	1112	1112	1112	1112	NC17 s(11) N1C s(10) C2C6 s(10)
		1097	1097	1097	1097	NC17 s(22) $C12H_2$ tw(12) NC11 s(11) CC14 s(10)
1074 mw	1074 s	1068	1068	1068	1068	C6C7 s(22) C2C6 s(20) $C6H_2$ r(11)
1041 ms	1046 sh	1052	1053	1052	1053	$C17H_2$ r(41) CO19 ob(19) COH b(13)

Table VI (*Continued*)

Observed[a]		Calculated				
Raman	IR	A	B_1	B_2	B_3	Potential Energy Distribution[b]
1029 sh	1030 w	1028	1024	1028	1024	COH b(45) CO20 t(13)
1014 ms	1013 mw	1004	1007	1004	1007	CC12 s(14) CSH b(13)
989 mw	989 sh	998	998	998	998	CC12 s(24) $C6H_2$ r(14)
953 mw	951 w	956	956	956	956	$C7H_2$ r(27) CSH b(12) N1C s(12)
930 ms	930 m	927	927	927	927	CSH b(25) $C7H_2$ r(19) NC11 s(12) N1C s(10)
917 m	917 w	905	905	905	906	C8N s(10)
885 s	884 vw	892	890	890	892	CC3 s(41) C6C7 s(14)
868 m	867 w	873	871	873	871	C14N s(11) CC8 s(11)
		863	865	863	865	CO20 s(29) C17C s(26) COH b(14)
828 ms	828 m	828	821	828	821	COH b(16) NC17C d(10)
812 mw	811 w	811	810	810	811	N1C s(25) $C6H_2$ r(18)
775 m		786	786	786	786	CO_2 b(34) CO_2 w(23) CO_2 ss(18)
	764 m	763	761	763	761	$C12H_2$ r(20) CSH b(15)
756 sh	759 sh	745	744	745	744	$C12H_2$ r(39) CSH b(14)
722 w	720 mw	723	723	723	723	CO_2 b(24) CO_2 w(17)
		704		704		C14N t(41) COH b(16) OH···O b(11) N16H ob(10) C8N t(10)
	691 m		700		700	C14N t(49) C8N t(21) N16H ob(13)
			692		692	C8N t(34) C14N t(23) N16H ob(18)
		691		691		C8N t(52) C14N t(16) N10H ob(13) N16H ob(12)
679 vs	682 sh		679		679	CS s(46) C8N t(19) C14O ob(12) N10H ob(11)
		678		678		CS s(55) C14O ob(12) C8N t(10)
659 w	657 w	648		648		C8O ob(17) OH···O b(11) COH b(11) N10H ob(11) CO20 t(10)
			649		649	CS s(19) N10H ob(13) C8O ob(11)
642 vw	643 m	642	643	642	643	CC8 s(10)
624 s	617 m	625	624	625	624	C8O ob(24) CC7C d(15) CCO20 d(15) CO20 t(12) COH b(10) OH···O b(10)
		588	592	588	592	CO19 ob(18) C8O ib(14) C8O ob(14) $C17H_2$ r(13) CC8 s(10)
			569		569	CC8N d(19) N1C t(10)
		565		566		CC8N d(19) C14O ib(12)
548 m	550 s	556	555	557	554	N1C t(27)
		544		544		C8O ob(14) N1C t(12) NCC14 d(11)
			548		547	C8O ob(15) N1C t(13) CO19 ob(12)
518 w	522 w	531	531	531	531	CO_2 r(31) N1C s(30)
			498		498	COH b(31) CO19 ib(29) OH···O b(25) CO20 t(15)
477 w	478 m	487		487		COH b(33) CO19 ib(29) OH···O b(27) CO20 t(16) C14N t(15) CO19 ob(14) $C17H_2$ r(11)
446 w		444	446	445	445	CC6C d(21) CC7C d(20)
429 vw			423		423	C12 b1(14) CCO20 d(14) CCS d(10)
		418		417		CCO20 d(17) N16H ob(12) C12 b1(12) CO19 ib(11)
401 vs		406	404	404	406	C3 b2(22) NCC3 d(19) CO_2 r(13) C3 b1(13)
360 sh		351	355	352	354	C12 b2(21) C12 b1(10) CC14N d(10) C14O ib(10)
350 m		343	331	343	331	CCO20 d(27) NC17C d(17)
303 m			297	299		NCC3 d(15) CN16C d(12)
		294			292	CN16C d(20) NCC3 d(11)
		282	281	282	281	SH···O b(77)
		267	273	273	267	C3 b1(19) NCC3 d(13) CN16C d(12) CO_2 r(10)
		260	261	260	261	C12 b2(32)
		246	242	241	247	C3 b1(37)
		213	214	213	214	CC14N d(14) CN16C d(11) N10H ob(10)
		205	207	207	205	C3 b2(22) CN10C d(13) CC6C d(11) CC14N d(11)
		179	179	179	180	CN10C d(27) CCS d(20)

[a] s, Strong; m, medium; w, weak; sh, shoulder.

[b] Contributions to potential energy distribution of 10 or larger. s, Stretch; ss, symmetric stretch; as, antisymmetric stretch; b, bend; sb, symmetric bend; ab, antisymmetric bend; ib, in-plane bend; ob, out-of-plane bend; d, deformation; w, wag; tw, twist; r, rock; t, torsion.

Table VII Observed and Calculated Frequencies (in cm^{-1}) of GSD

Observed[a]		Calculated				
Raman	IR	A	B_1	B_2	B_3	Potential Energy Distribution[b]
		3022	3022	3022	3022	$C17H_2$ as(77) $C17H_2$ ss(22)
2997 w		2995	2995	2995	2995	$C7H_2$ as(60) $C6H_2$ as(39)
2989 w	2988 w	2992	2992	2992	2992	$C6H_2$ as(60) $C7H_2$ as(39)
2970 sh	2970 w	2979	2979	2979	2979	$C12H_2$ as(100)
2949 vs	2948 mw	2953	2953	2953	2953	$C17H_2$ ss(78) $C17H_2$ as(24)
	2940 sh	2937	2937	2937	2937	$C12H_2$ ss(100)
2909 w	2907 w	2928	2928	2928	2928	$C6H_2$ ss(71) $C7H_2$ ss(28)
		2925	2925	2925	2925	$C7H_2$ ss(72) $C6H_2$ ss(28)
	2865 w	2866	2866	2866	2866	C2H s(99)
		2864	2864	2864	2864	C11H s(99)
	2495 ms	2462	2462	2462	2462	N10D s(98)
	2434 w	2443	2443	2443	2443	OD s(108)
	2396 m	2403	2402	2403	2402	N16D s(97)
	2346 m	2316	2316	2316	2316	ND_3 as1(74) ND_3 as2(24)
		2310	2310	2310	2310	ND_3 as2(74) ND_3 as1(24)
	2189 w	2174	2174	2174	2174	ND_3 ss(98)
1865 w		1821	1821	1821	1821	SD s(100)
1837 m	1837 m					
1708 w	1713m	1709	1709	1709	1709	CO19 s(93) CCO20 d(10)
1655 s	1656 s	1657	1652	1657	1658	C8O s(71) C8N s(24) CC8N d(10)
1620 s	1623 sh	1622	1624	1622	1623	C14O s(74) C14N s(26)
	1604 vs	1602	1602	1602	1602	CO_2 as(101) CO_2 r(11)
1486 m	1485 m	1492	1492	1492	1492	C14N s(31) CC14 s(28) C14O ib(18) N16D ib(12) NC17 s(11)
1466 m	1464 ms	1471	1471	1471	1471	$C7H_2$ b(25) CC8 s(22) C8N s(17) C8O ib(11)
		1450	1450	1450	1450	$C6H_2$ b(71) C2C6 s(10)
1445 m	1445 w	1444	1444	1444	1444	$C12H_2$ b(92)
	1439 sh	1440	1440	1440	1440	$C17H_2$ b(90)
		1422	1422	1422	1422	$C7H_2$ b(65) C8N s(10)
1411 s	1412 mw	1401	1401	1401	1401	CO_2 ss(39) CC3 s(24) CO_2 ib(22) $C6H_2$ w(11) $C6H_2$ b(10)
1399 w	1397 m	1393	1393	1393	1393	$C6H_2$ w(27) CO_2 ss(22) CO_2 ib(12)
1350 w	1349 m	1360	1362	1360	1362	$C17H_2$ w(48) C17C s(23) CO20 s(18)
		1339	1339	1339	1339	H^{α}[C2] b2(33) $C7H_2$ w(24) $C6H_2$ tw(23)
1332s	1331 s	1323	1321	1323	1321	$C17H_2$ w(39) CO20 s(36) CO19 ib(18)
1319 w	1316 mw	1320	1320	1320	1320	H^{α}[C2] b2(37) $C6H_2$ tw(15) $C7H_2$ w(13) $C7H_2$ tw(10)
1293 mw	1289 sh	1294	1294	1294	1294	H^{α}[C11] b2(78)
1276 m	1273 m	1270	1271	1270	1271	$C17H_2$ tw(87)
1249 w		1262	1262	1262	1262	$C12H_2$ w(44) H^{α}[C11] b1(29)
	1239 w	1258	1258	1258	1258	$C7H_2$ w(26) H^{α}[C2] b1(22) $C7H_2$ tw(19) $C6H_2$ tw(12)
1227 w	1225 mw	1224	1224	1224	1224	$C6H_2$ tw(18) $C7H_2$ tw(17)
	1213 w	1216	1216	1216	1216	$C12H_2$ tw(47) NC11 s(11)
1195 vw	1194w	1202	1202	1202	1202	ND_3 r2(19) C2C6 s(17) H^{α}[C2] b1(14) $C6H_2$ w(13)
1186 vw	1182 s	1180	1180	1180	1180	$C12H_2$ w(40) H^{α}[C11] b1(36)
		1155	1155	1155	1155	ND_3 ab1(31) ND_3 ab2(17) $C7H_2$ tw(13)
		1151	1151	1151	1151	H^{α}[C2] b1(28) ND_3 ab2(27) $C7H_2$ tw(11) $C6H_2$ w(10)
1129 w	1134 m	1126	1126	1126	1126	$C6H_2$ r(9) ND_3 sb(8)
1117 m	1117 sh	1116	1116	1116	1116	ND_3 ab1(18) NC17 s(14) ND_3 ab2(11) H^{α}[C11] b1(10)
		1115	1115	1115	1115	ND_3 ab1(20) ND_3 ab2(19) C2C6 s(11)
1098 mw	1098 mw	1090	1090	1090	1090	ND_3 sb(15) NC17 s(14) NC11 s(12) $C12H_2$ tw(12)
1062 m	1063 s	1068	1069	1068	1069	$C17H_2$ r(26) N16D ib(15) CO19 ob(13) ND_3 sb(11)
		1066	1066	1066	1066	ND_3 sb(38)
	1051 mw	1035	1035	1035	1035	N10D ib(17) ND_3 sb(11)
1028 vw	1029 mw	1026	1026	1026	1026	ND_3 r1(22) N10D ib(13)
998 sh	1000 vw	1004	1004	1004	1004	C6C7 s(24) CC12 s(17)
982 m		982	980	982	980	N16D ib(34) $C17H_2$ r(13)
959 s	959 s	962	962	962	962	CC12 s(20) N16D ib(16) N10D ib(12) $C7H_2$ r(11)
948 sh		941	941	941	941	$C7H_2$ r(24) N1C s(21)
920 m	919 mw	914	914	914	913	ND_3 r2(31)

Table VII (*Continued*)

Observed[a]		Calculated				
Raman	IR	A	B_1	B_2	B_3	Potential Energy Distribution[b]
909 vw	908 mw		891		891	CO20 s(18) COD b(11) C17C s(11)
		888		888		CO20 s(28) COD b(16) C17C s(16)
885 w	888 sh	882		882		C8N s(11)
			877		877	CO20 s(15)
861 m	859 mw	867	868	867	868	NC11 s(18) $C12H_2$ r(15)
842 w	843 w	848	847	845	848	CC3 s(29) ND_3 r1(19) C2C6 s(10)
831 mw	831 ms	844	844	843	846	$C12H_2$ r(22) C14N s(10)
		813	809	813	809	NC17C d(15) C17C s(11)
804 w	803 w	800	799	799	800	N1C s(27) $C6H_2$ r(13) CO_2 b(10) CO_2 w(10)
785 mw	785 vw	783	784	784	783	CO_2 b(29) CO_2 w(27) CO_2 ss(15)
755w	754 m	749	750	749	750	COD b(10)
728 w	727 m	706	706	706	706	CO_2 b(22) CO_2 w(15) CC3 s(12)
681 vs	679 sh	683	682	683	682	CS s(32) COD b(27)
	672 w	680	678	680	678	COD b(32) C14O ob(18) $C17H_2$ r(10) CO19 ob(10)
649 sh	645 sh	655	651	655	651	CS s(35)
	633 ms	635	635	635	635	C8O ob(35) CC7C d(25) C8O ib(11) CC8 s(10)
625 sh	626 vw	619	619	619	619	CSD b(78) $C12H_2$ r(23)
614 ms	610 ms	596	595	596	595	CCO20 d(18) $C17H_2$ r(16) CO19 ob(15) NC17C d(12) CO20 t(11)
571 vw		586	587	586	587	C8O ob(20) C8O ib(14) CC8 s(11) CO19 ib(11)
		556	556	556	557	CC8N d(18) C14O ib(18) C8O ib(10)
543 sh		534	540	534	540	NC11C d(16)
533 mw	528 s	525	523	523	525	CO_2 r(35) N1C s(32) C8N t(10)
515 sh		505	500	505	500	C14N t(48) COD b(25) N16D ob(19) OD···O b(18) CO20 t(14)CO20···D b(12)
480 vw		492	491	491	492	C8N t(70) N10D ob(33) O5···D3[N1] s(10)
468 sh	469 m	451	450	451	450	CC7C d(19) CC6C d(16) N10D ib(10)
445 vw			436		436	COD b(61) OD···O b(54) CO20 t(42)
		429		429		COD b(37) OD···O b(33) CO20 t(25)
418 vw			420		420	CCO20 d(13) C12 b1(12) CCS d(10)
		405		404		N16D ob(25) CO19 ib(20) C14N t(19) CCO20 d(15) COD b(10)
399 m		394	396	396	395	N1C t(20) C3 b2(13) NCC3 d(12)
		386	385	384	386	N1C t(29) C3 b2(10) NCC3 d(10)
362 w		346	351	348	350	C12 b2(18)
339 w		334	320	334	320	CCO20 d(26) NC17C d(16) C12 b2(11)
305 w		290	289	292	286	CN16C d(24) NCC3 d(10)
		261	265	266	261	CC7C d(13) NCC3 d(12) CN16C d(12)
		255	257	256	256	C12 b2(28)
		233	230	230	233	C3 b1(57) CO_2 w(10)
		211	213	211	213	SD···O b(12) CC14N d(11) CN16C d(10)
		203	204	204	203	SD···O b(14) CC14N d(13) C3 b2(13) CN10C d(11)
		198	198	198	198	SD···O b(63)
		176	176	176	177	CN10C d(24) CCS d(19)

[a] s, Strong; m, medium; w, weak; sh, shoulder.
[b] Contributions to potential energy distribution of 10 or larger, s, Stretch; ss, symmetric stretch; as, antisymmetric stretch; b, bend; sb, symmetric bend; ab, antisymmetric bend; ib, in-plane bend; ob, out-of-plane bend; d, deformation; w, wag; tw, twist; r, rock; t, torsion.

contribution is predicted for a mode at 864 cm^{-1}, and a Raman band at 868 cm^{-1} is assignable to this mode. In GSD this mode is predicted to move down, with a major CO20 s contribution at 1322 (1332) cm^{-1} and a smaller contribution at 1361 cm^{-1}, which may be assignable to the 1349 cm^{-1} band. This situation illustrates the value of having ab initio force fields derived from higher energy-minimum structures of small molecules that model the comparable part of a larger molecule.

The other bands in this region are associated with modes that are generally complex combinations of $C^{\alpha}H^{\alpha}$ b, NH ib, CH_2 w, and CH_2 twist (tw), with NH_3^+ rock (r) occasionally mixed in. There is no CN s contribution ≥5, except for C8N s (7) in the 1300 cm^{-1} mode, so no traditional amide III modes

exist for GSH. Significant NH ib contributions occur for predicted modes at ~ 1337, 1321, and 1254 cm^{-1}, for which there are assignable bands at ~ 1335, 1310, and 1249 cm^{-1}, but while the second and third of these disappear on deuteration, and make expected contributions at 1068 (1063), 1035 (1051), 1026 (1029), 981 (982), and 962 (959) cm ^{1}, the first does not because it retains its essential CO20 s character, at 1322 (1332) cm^{-1}. The Gly $C17H_2$ w modes at 1368 and ~ 1318 cm^{-1} in GSH, assignable to bands at 1368 and 1310 cm ^{1}, seem to diminish their separation in GSD to modes at 1361 and 1322 cm ^{1}; this suggests, considering a possible further reduced splitting (from the supposedly parent frequency near 1343 cm ^{1}), the assignment to bands at 1349 and 1332 cm^{-1} in GSD. The $C17H_2$ tw mode at 1275 (1280) cm^{-1} in GSH shifts slightly to 1271 (1275) cm^{-1} in GSD. The Cys $C12H_2$ w, H$^{\alpha}$[C11] b1 modes remain relatively unchanged: 1260 (1255) and 1174 (1170) cm^{-1} in GSH, 1262 (1249) and 1180 (1182) cm^{-1} in GSD. The $C12H_2$ tw mode at 1201 (1200) cm^{-1} in GSH increases in GSD to 1216 (1213) cm^{-1}, while a H$^{\alpha}$[C11] b1, $C12H_2$ tw mode at 1125 (1122) cm^{-1} retains some of this character in GSD at 1126 (1129) cm ^{1}. The remaining $C6H_2$ and $C7H_2$ w and tw contributions (mixed with some H$^{\alpha}$ b) are well accounted for: 1355 (1351), 1300 (1290), 1252 (1249), 1217 (1224), and 1149 (1143) cm^{-1} in GSH with similar contributions but different H$^{\alpha}$ b admixtures at 1339 (1349), 1320 (1318), 1258 (1239), 1224 (1226), and 1151 (—) cm^{-1} in GSD. The NH_3 r coordinates contribute to bands at 1342 (1342), 1291 (1290), and 1241 (1235) cm^{-1} in GSH, and their counterparts in GSD seem to be well accounted for at 1202 (1195), 1026 (1029), and 914 (920) cm^{-1}. Predominant H$^{\alpha}$ b contributions in GSH modes remain in GSD, although in some cases large changes occur in mode composition: 1342 (1342) to 1320 (1318), 1300 (1290) to 1294 (1293), 1254 (1249) to 1258 (1239), 1174 (1170) to 1180 (1182), 1149 (1143) to 1151 (—), and 1125 (1122) to 1116 (1117) cm ^{1}. It is clear that a very complex mixing of coordinates occurs in the normal modes in this region, and simplified designations such as amide III are totally unwarranted. Reality usually requires a more sophisticated view of normal modes of complex molecules.

1100–700 cm^{-1} Region

This region contains the expected skeletal stretch and CH_2 r modes as well as COH b, CSH b, and CO_2 deformation modes. This leads to significant mixing of these coordinates in most of the modes, with large changes in GSD because of the new mixing with ND ib and ND_3 r modes.

About the only skeletal modes to retain their essential character and localized frequency are N1C s, which can be assigned at 811 (812) cm ^{1} in GSH and 800 (804) cm ^{1} in GSD, and NC17 s, assignable to 1097 (—) cm^{-1} in GSH and 1090 (1098) cm^{-1} in GSD, with the latter probably gaining intensity from its ND_3 sb component. The C17C s mode retains its main form but shifts from 864 (868) cm ^{1} in GSH to 890 (908) cm ^{1} in GSD because of the replacement of COH b by COD b. Others retain the major skeletal component but change significantly in character and frequency: CC3 s at 891 (885) cm^{-1} in GSH and 847 (843) cm^{-1} in GSD; C6C7 at 1068 (1074) cm ^{1} in GSH and 1004 (1000) cm^{-1} in GSD; and CC12 s at 1006 (1014) cm^{-1} in GSH and 962 (959) cm^{-1} in GSD. Except for C2C6 s, which changes from a major component at 1068 (1074) cm ^{1} in GSH to a minor component at 847 (843) cm^{-1} in GSD, and NC11 s, which is distributed in minor proportions at 1125 (1122), 1097 (—), and 927 (930) cm ^{1} in GSH and is concentrated at 868 (860) cm ^{1} in GSD, the remaining skeletal stretch coordinates represent small contributions in GSH that either remain small in GSD [cf. C8N s at 905 (917) and 882 (885) cm^{-1}; and C14N s at 872 (868) and 844 (831) cm^{-1}] or drop below our PED limit of 10 in GSD [cf. CC8 s at 872 (868) cm ^{1} and CC14 s at 1097 (—) cm ^{1}].

Similar complex behavior is observed in the CH_2 r modes. The $C6H_2$ r coordinate, which in GSH is distributed between three modes at 1068 (1074), 998 (989), and 811 (812) cm ^{1}, becomes concentrated in GSD at 800 (804) cm ^{1}. The $C7H_2$ r coordinate mixes with CSH b in GSH to give two modes at 956 (952) and 927 (930) cm^{-1} and is concentrated in GSD at 941 (948) cm^{-1}. The $C17H_2$ r coordinate, which in GSH is concentrated in a mode at 1053 (1041), with a small contribution at 590 (—) cm ^{1}, becomes dispersed in GSD to modes at 1069 (1063), 981 (982), 679 (672), and 596 (612) cm^{-1}. The Cys $C12H_2$ r mode, which is found in ethanethiol at 737 cm ^{1},[12] is split in GSH between modes at 762 (764) and 745 (758) cm ^{1}, but is further separated in GSD to modes at 868 (860), 844 (831), and 619 (626) cm^{-1}.

As we noted above, the COH b force constant was determined by the requirement that CO19 s and CO20 s not shift on deuteration. This results in significant COH b contributions at 1026 (1030), 864 (868), 825 (828), and 492 (478) cm^{-1} in GSH and COD b at 888 (908), 683 (681), 679 (672), 503 (515), and 433 (445) cm ^{1} in GSD. Assignments

based on simple disappearance of bands on deuteration are not feasible in this case because of the presence in GSD of new modes at about the same positions [cf. 1029 cm^{-1}: ND_3 r1, N10D ib; 860 cm^{-1}: NC11 s, $C12H_2$ r; 831 cm^{-1}: $C12H_2$ r, C14N s; and 480 cm^{-1}: C8N t, N10D ob].

For the comparable conformation, CSH b in ethanethiol is found at 869 cm^{-1}.[12] In GSH we assign this mode to 927 (930) cm^{-1}, where it mixes with $C7H_2$ r and skeletal stretch coordinates. It is also found mixed with $C12H_2$ r at 762 (764) and 745 (759) cm^{-1}. In GSD this mode is concentrated at 619 (626) cm^{-1}, comparable to the 625 cm^{-1} band found in ethanethiol-SD.[12]

The remaining CO_2^- b, CO_2^- w modes in this region are reasonably well accounted for: 786 (775) and 723 (721) in GSH and 784 (785) and 706 (727) cm^{-1} in GSD.

Amide V and Skeletal Deformation Region

The amide V mode, CN torsion (t) plus NH ob, is usually strong in the ir and weak in the Raman, and these modes are well assigned in GSH to bands at 702 (691) and 692 (691) cm^{-1}. They disappear in GSD, and their counterparts at 503 (515) and 492 (480) cm^{-1} are very weak.

Other than the skeletal deformation modes, the CS s mode, which is a strong Raman band at 662 cm^{-1} in ethanethiol,[12] appears at 679 (679) cm^{-1} in GSH (mixed with amide V of C8N10), and its shift to 683 (681) cm^{-1} in GSD is well predicted. Another CS s contribution is present in the B_1 and B_3 modes at 649 (658) cm^{-1} [as well as a CS s (9) at 643 (643) cm^{-1}], and this appears at 653 (647) cm^{-1} in GSD. The same agreement holds for the NH_3^+ and CO_2^- end group modes: N1C t shifts from 556 (549) cm^{-1} in GSH to 395 (399) cm^{-1} in GSD, while CO_2 r at 531 (520) cm^{-1} in GSH remains relatively unchanged in GSD at 524 (528) cm^{-1}, although it perhaps gains intensity from a new C8N t contribution.

The skeletal deformation coordinates are significantly mixed throughout this region, with only some patterns evident. While CO19 ob contributes at higher frequencies, at 1053 (1041) cm^{-1} in GSH and 1069 (1063) cm^{-1} in GSD, as well as at lower frequencies, 590 (—) cm^{-1} in GSH and 596 (612) cm^{-1} in GSD, C14O ob and C8O b contribute only in the lower frequency region. However, C14O ob mixes with CS s in GSH, at 679 (679) cm^{-1}, while in GSD it mixes predominately with COD b, at 679 (672) cm^{-1} [there is a C14O ob (9) contribution to the 683 (681) cm^{-1} mode]. On the other hand, C8O ob is dominant in three modes in GSH, at 648 (658), 625 (624), and 546 (549) cm^{-1}, retaining this dominance in two modes in GSD, at 635 (633) and 587 (571) cm^{-1}. A CC6C deformation (d), CC7C d mode at 445 (446) cm^{-1} in GSH moves to 451 (469) cm^{-1} in GSD, perhaps gaining intensity from an N10D ib contribution. The CCO20 d coordinate contributes to bands at 420 (429) and 337 (350) cm^{-1} in GSH, with contributions at 412 (418) (modified by N16D ob) and 327 (339) cm^{-1} in GSD. A strong band at 401 cm^{-1} in GSH can be assigned to C3 b2, NCC3 d, with a counterpart in GSD at 395 (399) cm^{-1}. The C12 b2 mode is at 353 (360) in GSH and at 349 (362) in GSD, and a CN16C d mode stays relatively constant at 296 (303) in GSH and 289 (305) cm^{-1} in GSD.

CONCLUSIONS

The GSH molecule presents a challenging problem in normal mode analysis because of the variety of different chemical groupings of atoms in its structure: main-chain peptide groups, charged NH_3^+ and CO_2 end groups, uncharged side-chain (CH_2SH) and end (CH_2COOH) groups, and an unusual main-chain (γ-Glu) structure. In addition, all of the capable groups participate in a complex pattern of hydrogen bonds between the four molecules in the unit cell. Nevertheless, using currently available empirical force fields for the peptide group[8] and the charged end group,[9-11] together with ab initio force fields for the CH_2SH and CH_2COOH moieties, it has been possible to obtain very good agreement between calculated and observed frequencies for GSH (the average error for observed bands is about 5 cm^{-1}) and to satisfactorily account for observed shifts in the deuterated GSD molecule. This not only enhances confidence in the force fields used, but suggests that these force fields should be substantively applicable to other conformations of this molecule.

More general normal mode treatments of multiple conformations of a molecular system will depend on having reliable conformation-dependent force fields. These will probably be based on molecular mechanics potentials, which we have shown can be rigorously derived from spectroscopic force fields,[26] i.e., sets of quadratic force constants, whether empirical or scaled ab initio, optimized to observed spectra. This approach has been applied to *n*-alkane chains,[27] and is now being extended to peptides.

This research was supported by NSF grants MCB-9115906 and DMR-9110353.

REFERENCES

1. Dolphin, D., Avramovic, O. & Poulson, R., Eds. (1989) *Glutathione: Chemical, Biochemical and Medical Aspects. Part A,* Wiley, New York.
2. Baillie, T. A. & Statter, J. G. (1991) *Acct. Chem. Res.* **24,** 264–270.
3. Wright, W. B. (1958) *Acta Cryst.* **11,** 632–643.
4. Görbitz, C. H. (1987) *Acta Chem. Scand.* **B41,** 362–366.
5. Huber, R. E. & Edwards, L. A. (1989) in *Glutathione: Chemical, Biochemical and Medical Aspects. Part A,* Wiley, New York, chap. 2.
6. Rabenstein, D. L. & Keire, D. A. (1989) in *Glutathione: Chemical, Biochemical and Medical Aspects. Part A,* Wiley, New York, chap. 3.
7. Laurence, P. R. & Thomson, C. (1980) *Theor. Chem. Acta* **57,** 25–41.
8. Krimm, S. & Bandekar, J. (1986) *Adv. Protein Chem.* **38,** 181–364.
9. Bandekar, J. & Krimm, S. (1988) *Biopolymers* **27,** 885–908.
10. Sundius, T., Bandekar, J. & Krimm, S. (1989) *J. Mol. Struct.* **214,** 119–142.
11. Qian, W., Bandekar, J. & Krimm, S. (1991) *Biopolymers* **31,** 193–210.
12. Qian, W. & Krimm, S. (1992) *Biopolymers* **32,** 1503–1518.
13. Qian, W. & Krimm, S., to be published.
14. Qian, W., Zhao, W. & Krimm, S. (1992) *J. Mol. Struct.* **250,** 89–102.
15. Cheam, T. C. & Krimm, S. (1989) *J. Mol. Struct. (Theochem.)* **188,** 15–43.
16. Reisdorf, W. C., Jr. (1994) Ph.D. thesis, University of Michigan.
17. Sengupta, P. K., Krimm, S. & Hsu, S. L. (1984) *Biopolymers* **23,** 1565–1594.
18. Susi, H., Byler, D. M. & Gerasimowicz, W. V. (1983) *J. Mol. Struct.* **102,** 63–79.
19. Kuczera, K. & Czerminski, R. (1983) *J. Mol. Struct.* **105,** 269–280.
20. Krimm, S. & Abe, Y. (1972) *Proc. Natl. Acad. Sci. USA* **69,** 2788–2792.
21. Moore, W. H. & Krimm, S. (1975) *Proc. Natl. Acad. Sci. USA* **72,** 4933–4935.
22. Krimm, S. & Dwivedi, A. M. (1982) *J. Raman Spectrosc.* **12,** 133–137.
23. Cheam, T. C. & Krimm, S. (1986) *J. Mol. Struct.* **146,** 175–189.
24. Snyder, R. G., Hsu, S. L. & Krimm, S. (1978) *Spectrochim. Acta* **34A,** 395–406.
25. Fraser, R. D. B. & Price, W. C. (1952) *Nature* **170,** 490–491.
26. Palmö, K., Pietilä, L.-O. & Krimm, S. (1991) *J. Comput. Chem.* **12,** 385–390.
27. Palmö, K., Mirkin, N. G., Pietilä, L.-O. & Krimm, S. (1993) *Macromolecules* **26,** 6831–6840.

Received February 25, 1994
Accepted April 25, 1994